Thermal Science and Engineering Progress 49 (2024) 102466

Contents lists available at ScienceDirect

Thermal Science and Engineering Progress

journal homepage: www.sciencedirect.com/journal/thermal-science-and-engineering-progress

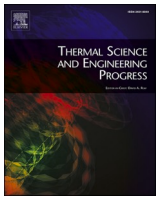

The effect of adsorption bed design optimization on COP and SCP system: Comparison for three couples' zeolite/water, silica gel/water and NH_2-MIL125/water

Oussama Ayed [a,*], Sébastien Thomas [b], Philippe André [b], Abdelmajid Jemni [a]

[a] Laboratory of Thermal and Energetic Systems Studies (LESTE), National School of Engineering of Monastir, University of Monastir, Tunisia
[b] Building Energy Monitoring and Simulation (BEMS), University of Liège, Belgium

ARTICLE INFO

Keywords:
Adsorption cooling system
Zeolite
Silica gel
NH_2-MIL125
Fins Design

ABSTRACT

In this study, three-dimensional numerical models of cylindrical adsorber were developed for vertical and horizontal fins. This adsorber contains fins filled with two traditional adsorbents (Zeolite and Silica gel) and a new adsorbent (NH_2-MIL125). The height of the adsorber is adjusted to have the same amount of the adsorbent for the different number of fins and adsorber design. The discretization of the coupled equations in the system is done by the finite volume method (FVM). The effect of the number and geometry of fins on the desorption kinetic and the specific cooling capacity are investigated for each one. The results showed that NH_2-MIL125 gives the best coefficient of performance (COP) and the highest Specific Cooling Power (SCP) comparing to the traditional adsorbents. For the vertical fins, results showed a low impact of the fins number and design of the different adsorbents (Zeolite, silica and NH_2-MIL125). This low impact is due to the configuration of the adsorbent bed. The factor form F is found to be correlated to the time cycle and the heat transfer. F has an optimal value of 0.4 when the number of fins is 15. The coefficient of performance (COP) shown to be independent from the fins number. The Specific Cooling Power (SCP) is affected by the fins number of the three adsorbents. NH_2-MIL125 is giving the best result of SCP reaching a value of 80 Wh/kg. Considering the obtained results, the NH_2-MIL125 is a promising adsorbent for the adsorption cooling system.

1. Introduction

After the Kyoto Protocol and recently the Paris Agreement, many countries have started taking steps to reduce their dependence on fossil fuels, that provide conventional energy resources which are not sustainable. The renewable energy sources are the remedy for this old energy sources. The use of renewable energy reduces the pollution and creates new fields of investment. The renewable energy secures the reduction of pollution and creates new field of investment to cover the demand of the population. Cooling system has a crucial importance in the human life, which is needed in all the vital areas, like food, agriculture, manufacturing, medical industries, preservation, air conditioning, ice making, etc. Meanwhile the traditional vapor compression systems lost its durability due to the high consumption of energy (almost 45 % of the house consumption of electricity) [1]. In addition, the used refrigerants Chlorofluorocarbons (CFCs) and Hydrochlorofluorocarbons (HCFCs) contribute to the pollution such as ozone depletion and climate change. Besides, it was proved that the CFCS/CFC are the origin of one third of the global greenhouse effect [2,3].

The adsorption cooling technology presents an attractive alternative to traditional systems. In fact, these are eco-friendly as refrigerants do not harm the environment such as water [4–9]. Moreover, they can be powered by low temperature driving sources such as solar heat, industrial/automobile waste heat and geothermal heat. The global waste heat is estimated as 72 % of the primary used energy [10]. Hassan et *al* [11,12] studied a new configuration system for the simultaneous production of electricity and cooling from solar energy. Compared with systems based on the Photovoltaic thermal collector (PVT) alone and on evacuated tube collectors (ETC-only) powered adsorption system, for the same area of the solar collector, the new configuration proposed proved to be the best performing, with a high energy efficiency.

However, the adsorption cooling technology does not meet yet the desired level as far as for their Coefficient of Performances (COP) and Specific Cooling Power density (SCP) comparing to the traditional cooling systems [13,14]. However, at low power levels, these adsorption

* Corresponding author.
E-mail address: ou_ayed@yahoo.fr (O. Ayed).

https://doi.org/10.1016/j.tsep.2024.102466
Received 17 September 2023; Received in revised form 29 January 2024; Accepted 15 February 2024
Available online 19 February 2024

Nomenclature

a_i	First term of Langmuir
b_i	Second term of Langmuir
COP	Coefficient of Performance
c_i	Langmuir third term
C_p	Specific heat in constant pressure J/(kg.K)
D	Diffusion coefficient m^2/s
E_a	Diffusion activation energy kJ /mol
E_i	The fourth term of Langmuir W/K
F	The factor form
H	Convective heat transfer coefficient W/(m.K)
h	Height m
L	Latent heat J/ kg
G	The mass transfer coefficient
K	Permeability m^2
$\dot{m}$	Mass flow rate Kg/ s
M	Molar mass of the water kg/mol
P	Pressure Pa
R	Perfect gas constant J/ (mol.K)
R_{in}	Inner radius m
R_{out}	Outer radius m
R_f	Fin radius m
R	Radial coordinate m
r_p	Adsorbent granule radius m
S	Solid/gas transfer area m^2/m^3
SCP	Specific Cooling Power Wh/kg
T	Temperature K
t	time S
V	Velocity m/s
X	Adsorbed amount Kg/kg_{ads}

Greek

ε	Total porosity
λ	Thermal conductivity W/(m.K)
μ	Dynamic viscosity kg /(m.s)
ρ	Density kg /m
ν	Kinematic viscosity m^2/s
ΔH	Heat of adsorption J/kg

Subscripts

R	Radial coordinate
z	Vertical coordinate
G	Gas
Sat	Saturation
Eq	Equilibrium
S	Solid
Ef	Effective
f	Fin

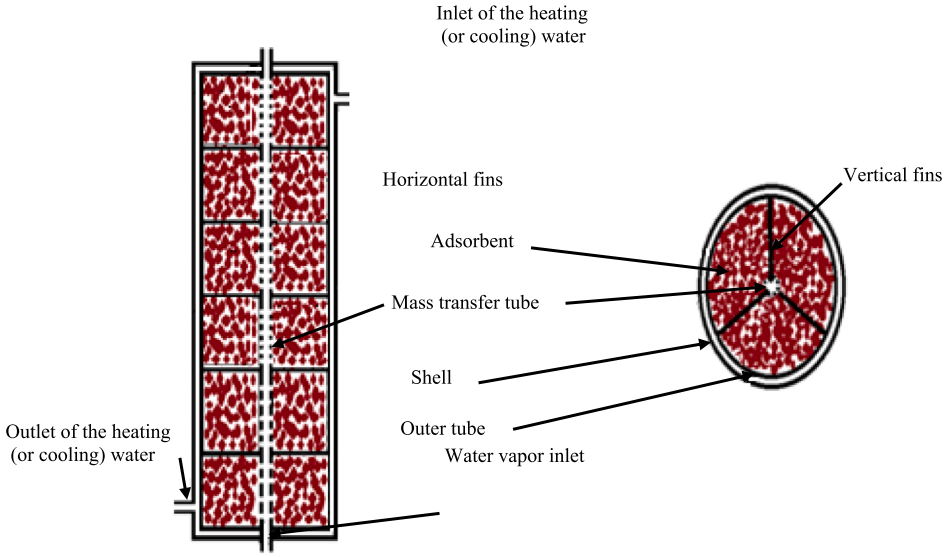

Fig. 1. Schematic view of the adsorption bed with horizontals and verticals fins.

Table 1
The Langmuir coefficients used by Ben Amar [43].

	A	C	b	E
0	0,152	−0,896	–	–
1	−155,36	843,85	$1{,}508\ 10^{-10}$	7726,58
2	$6{,}37\ 10^{4}$	$-2{,}54\ 10^{5}$	$5{,}417\ 10^{-10}$	6074,71
3	$-8{,}45^{6}$	$2{,}78\ 10^{7}$	$1{,}707\ 10^{-10}$	5392,17

Table 2
The constants of the isotherm equation [46].

	$NH_2MIL125$
A	0.23
B	0.025
E	0.425
F	–
G	0.97

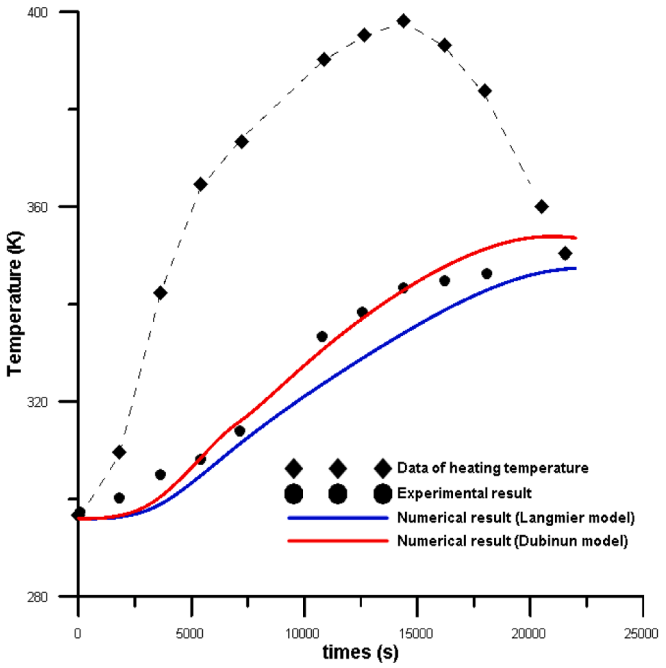

Fig. 2. Time evolution of the temperature on the inner and outer wall surface of the adsorber.

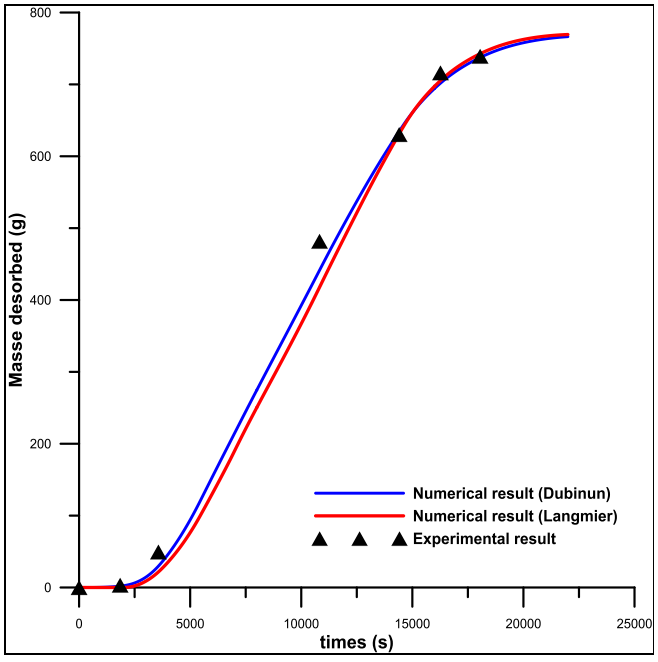

Fig. 3. Evolution of the desorbed mass.

Table 3
Temperature and the mass desorbed deviation compared to those in literature for both Langmuir and Dubinin numerical models.

	Langmuir model	Dubinin model
Mass desorbed (g)	8,93 %	7,77 %
Temperature (K)	0,75 %	1,71 %

refrigeration systems are more expensive than conventional systems of equivalent power. They also require a relatively large installation space. To increase the performance of the adsorption cooling system, the Coefficient of Performances (COP) and Specific Cooling Power (SCP) must be optimized. Therefore, a lot of studies are developed and continue to be developed to improve the performance by including a multiple stage cycle, heat, and mass recovery cycle, improving the characteristics of adsorbate-adsorbent couples and optimizing the adsorber bed heat exchangers [15]. Li et *al.* [16] studied the heat and mass transfer for two-dimensional quasi-equilibrium model in an annular finned tube silica gel module to identify the optimum fin pitch and height. It was concluded that without considering the effect of cycle time, the optimum fin spacing occurred was optimized between consecutive adsorption and desorption processes when the amount of refrigerant uptake by adsorbent. This result was only effective for optimizing the COP but not the SCP.

Leong and Liu [17] studied a simple adsorber tube chiller to see the effect of adsorbent parameters and adsorption bed such as porosity, adsorb particle size and bed height. It was demonstrated that elongate of the bed height increases the COP and reduces SCP. However, the porosity and particle size have a relatively small effect on the performance of the bed. Wang [18] used the equilibrium model as intra-particle mass transfer equation to investigate the effects of variety of parameters such as cooling and heating water temperature, heat and mass recovery time and cycle time. Kubota et *al.* [19] optimized the conditions of the adsorption chiller and tested the effect of cycle time, switching time and hot water temperature. They found that COP slightly improved with rising the hot water temperature. But the switching time had almost no effect on COP. Zhang and Wang [20] developed a numerical transient three-dimensional model of fin-tube type adsorption bed. They proved that there is an optimum fin dimension (with the highest values of COP and SCP. Saha et *al.* [21] modeled an adsorption bed for silica gel-water system with annular fins. They investigated the effect of cycle time, switching time and heating temperature on COP and cooling capacity. They found that COP is higher with larger cycle time and higher heating temperature. Moreover, the ultimate values of heating temperature, cycle time and switching time were found for cooling capacity. Pei-Zhi [22] reported that the extension of the time cycle leads to the augmentation of COP. But there is an optimal cycle time for the SCP. Niazmand et *al.* [23,24] investigated the processes of heat and mass transfer in a silica gel/water adsorption adsorber containing annular fins. Their studies proved that COP augmented, however SCP reduce when smaller particle sizes were used, larger fin pitch and larger fin height. Grabowska et *al.* [25,26] studied the effect of a coated sorbent layer on the heat transfer process in adsorption beds. The relationship of the bed structure and the adsorption pair was discussed.

Xiangbo [27] demonstrated that the COP decreased when the desorption time is extended due to the rising of the heat loss. The effect of fins height and spacing of a flat tube in adsorber were studied on the performance of a two-bed silica gel-water adsorption chiller using a lumped body mode (heating in range of 50–90 °C). Results showed that SCP could be increased up to 6.3 % and COP up to 3.7 % by the optimization of the fins geometry [28].

It was demonstrated by Verde et *al.* [29] that increasing the fins thickness and reducing its pitch enhance the SCP and the bed thermal conductance. New fins designs: rectangular and trapezoidal were used by Kowsari et et *al.* [30] showed that the rectangular form of fins gave the highest SCP comparing to the trapezoidal form, but the COP was the same for both cases.

Golparvar et *al.* [31] have developed a three-dimensional model to evaluate the effects of heat and mass transfer in longitudinal and annular finned tube filled with zeolite-13x adsorbent. The effect of the spacing of finned tube has been checked. The time cycle in this study was considered as twice the desorption time (adsorption time is equal to desorption time) and the tested adsorbent was only the Zeolite 13X. The aim of recent work is to develop new adsorption couples. L. Ye et *al* [32] have

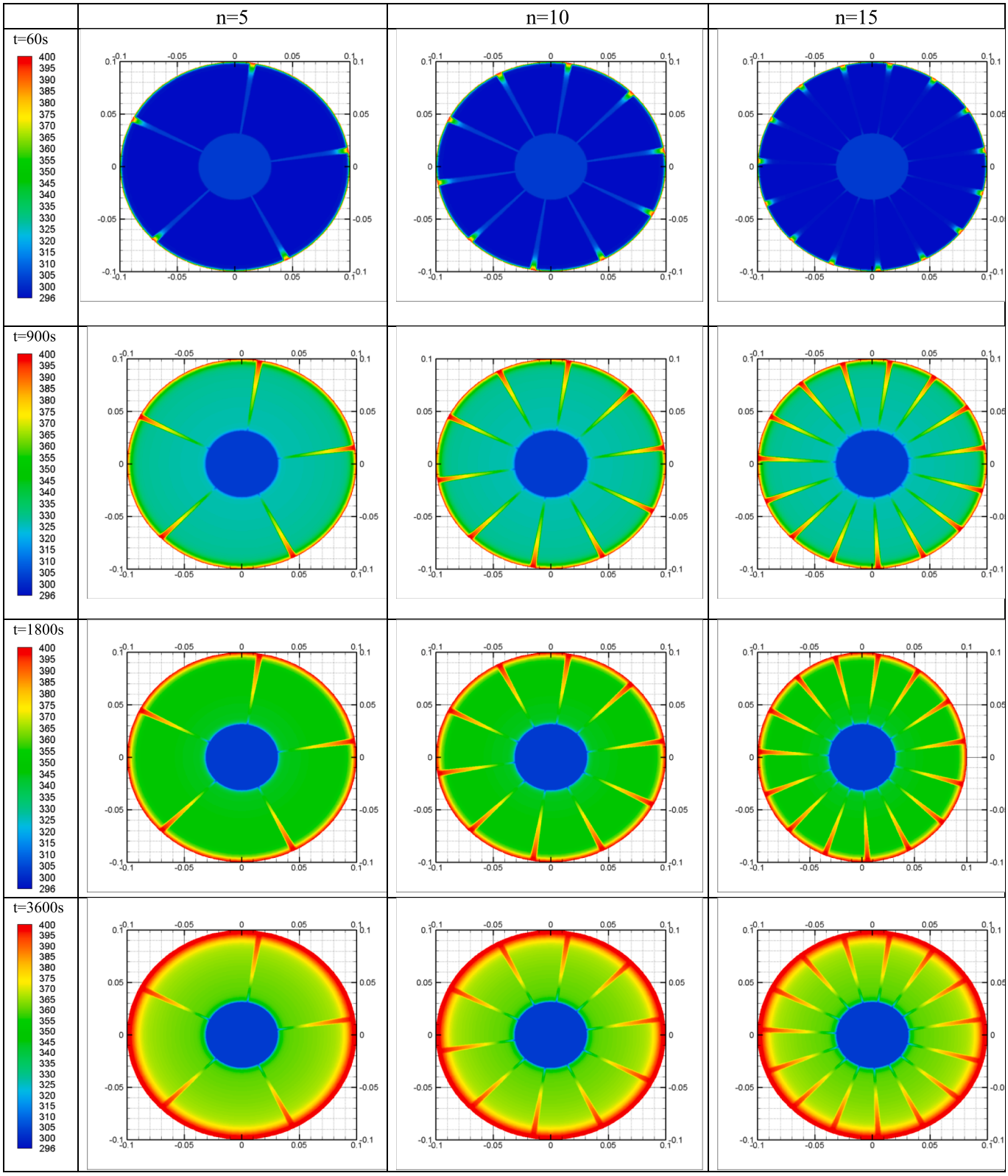

Fig. 4. Spatio-temporal evolution of the temperature in the desorption phase (vertical fins) when z = h/2.

used the Maxsorb III/HFO-1234ze(E) couple as a working couple. Theoretical and experimental studies have been carried out. The couple has been tested under different working conditions and the results are promising for the use of this couple in adsorption cooling systems.

New materials were developed the performance of adsorbent based on many focusing on Zeolite and silica gel. In fact, a variety of these composite were improved like SWS-1L by adding calcium chloride ($CaCl_2$) to mesoporous silica gel [33] or synthesized Zeolite like Zeolite 5A or 13X. Also new adsorbent type based on Zeolite, functional Adsorbent Material-Zeolite (FAM), is one of the new adsorbents for the heat pumps. Kakiuchi [34,35] introduced respectively FAM Z01 and Z02 with limited concentration of 0.2 and 0.3 kg/kg.

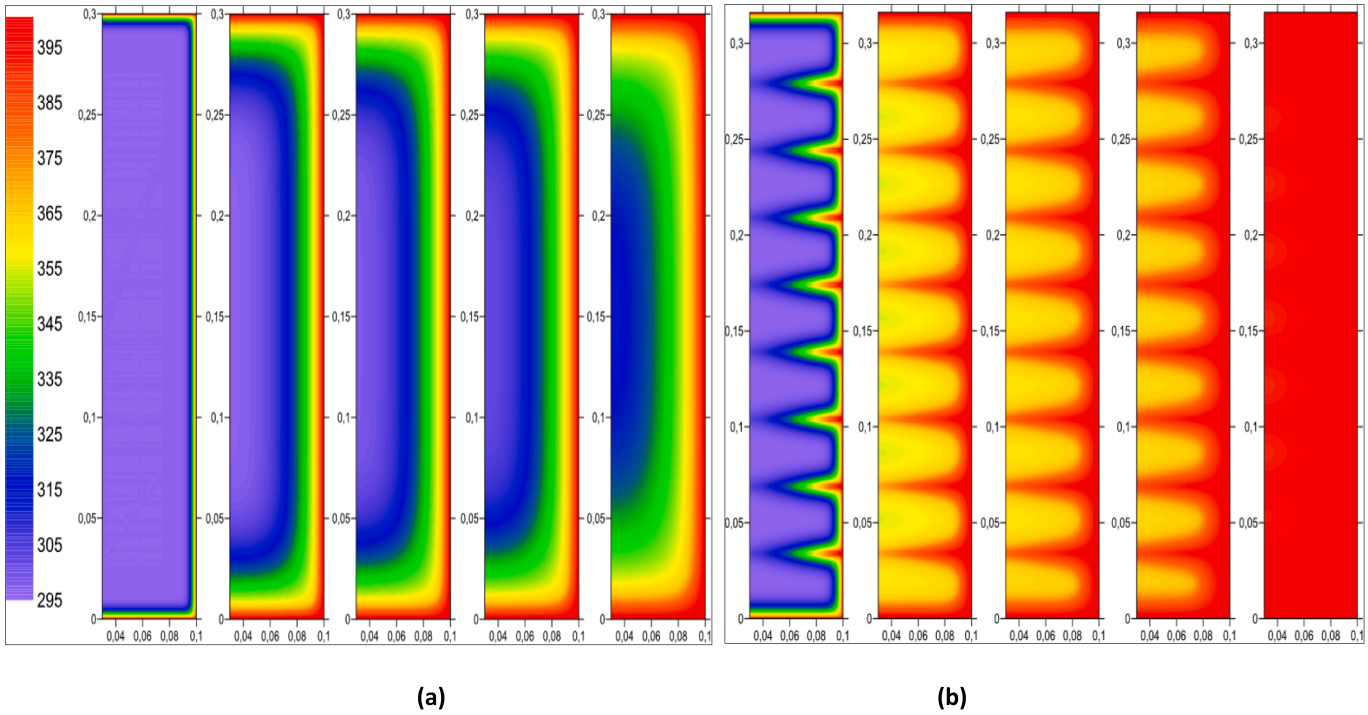

Fig. 5. A spatio-temporal temperature profile in a finless adsorber 6-b spatio-temporal temperature profile in an 8-finned adsorber (horizontal fins) (for t = 60 s,3600 s, 5400 s, 7200 s,14400 s).

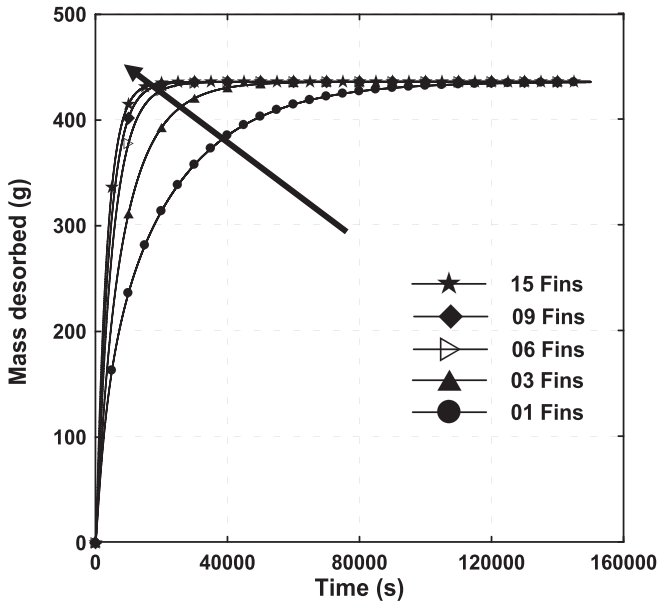

Fig. 6. Mass desorbed profile in term of horizontal fins.

Metal-organic frameworks (MOFs), which are characterized by their high adsorption capacity, can replace conventional adsorbent materials. Thanks to their high surface area, regular porosity and high crystallinity, which increase adsorption capacity, the MOF/water couple is an environmentally friendly adsorption couple [36–38]. NH_2-MIL-125 ($Ti_8O_8(OH)_4$-(O_2C-C_6H_5-CO_2-$NH_2)_6$) is another new composite for the adsorption heat pump. MIL-125 is a Ti-incorporated MOF structure [39]. After studying its effect on water adsorption, Gordeeva [40] showed that NH_2-MIL-125 could be a promising material for adsorptive heat transfer and storage. The measured parameters were the specific surface area, total, and micro-pore volumes of the composite.

The aim of this study is to present a 3D model developed which govern heat and mass transfer in an adsorber. This model was used to select the optimum geometric configuration of the adsorber and adsorbent for application in an adsorption cooling system. Three adsorbents were used, zeolite, silica gel and a new adsorbent NH_2-MIL125 in a cylindrical adsorption bed with horizontal and vertical fins. The SCP and COP of the refrigeration systems were calculated for each adsorbent for the different fins designs. The effect of factor form is studied to check the fin's effect in each bed configuration.

2. System description and methodology

2.1. System description

The considered physical model is shown in Fig. 1. It consists of three coaxial cylinders, the mass transfer tube, the outer tube, and the tubular shell. Even the mass transfer tube and the outer tube have the same height "h" and two different radiuses called the inner radius "R_{in}" and the outer radius "R_{out}", respectively. The radius and height of tubular shell are fixed to guarantee the heating (cooling) fluid flow at a constant fluid temperature T_{HF} over the entire exchange surface of the outer tube. The mass transfer tube exchanges the water vapor (adsorbate) with the condenser (evaporator). The annular space is devised by equidistant horizontal (vertical) fins made of copper. Their numbers, thickness and radius are variable. The adsorbent (Zeolite, silica gel or MIL125) is packed in the annulus between the mass transfer tube, the outer tube and the fins.

2.2. Mathematic model

The following assumptions were adopted for the formulation of heat and mass transfer equations in the studied bed,

- The adsorbate gas is assumed to be an ideal gas;
- The porous medium is isotropic and composed of uniformly sized particles.

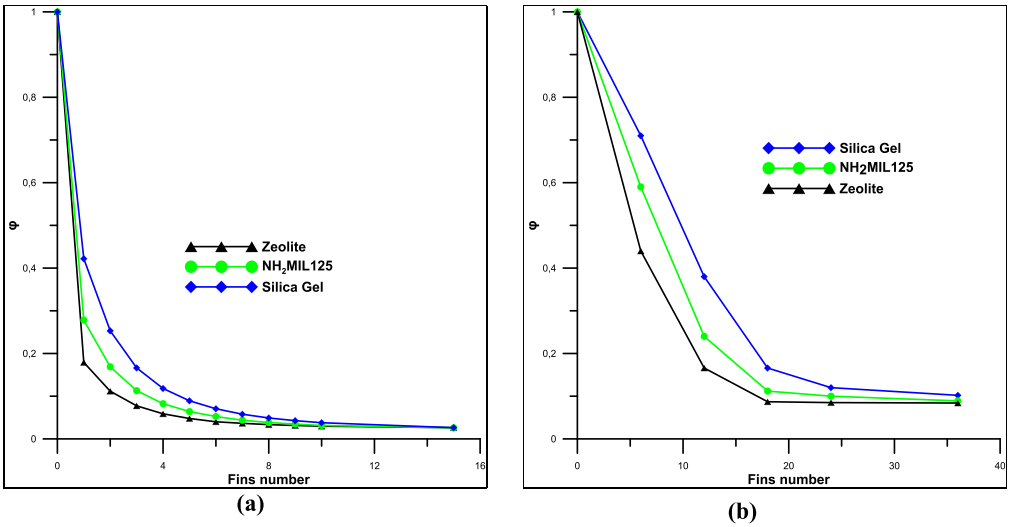

Fig. 7. φ profile in term of fins number; (a): horizontal fins, (b): vertical fins.

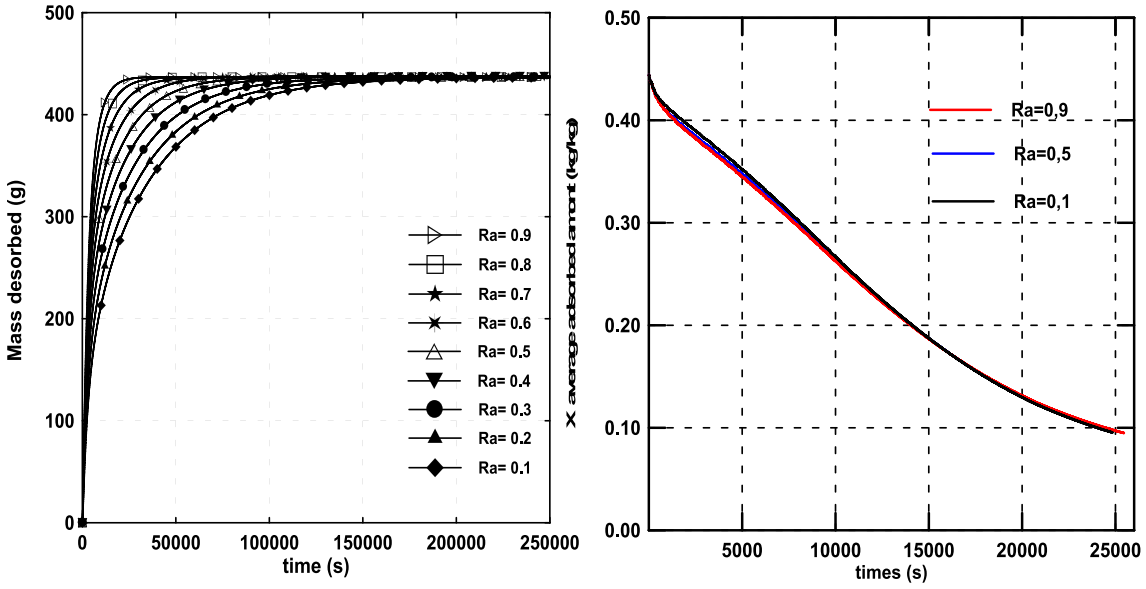

Fig. 8. Mass desorbed effect on the saturation time in term of fins radius.

- The porous medium particles are incompressible.
- The bed is assumed to be in local thermal equilibrium.
- The heat capacities of fluid and metal are considered constant.
- Darcy's law gives the gas flow rate.

2.2.1. Gas mass conservation equation

The mass conservation equation for the adsorbate in macro scale gas is written in cylindrical coordinates as:

$$\varepsilon\frac{\partial(\rho_g)}{\partial t}+\mathrm{div}\left(\rho_g V_g\right)+\dot{m}=0 \tag{1}$$

The Darcy's law expresses the vapour velocity as following:

$$\vec{V}=-\frac{K}{\mu_g}\overrightarrow{grad(P_g)} \tag{2}$$

The density of ideal gas is given by the following expression:

$$\rho_g=\frac{M}{RT_g}P_g \tag{3}$$

The rate of refrigerant adsorbed is defined as:

$$\dot{m}=-(1-\varepsilon)\rho_s\frac{\partial X}{\partial t} \tag{4}$$

Using equations (2) and (3), the equation (1) becomes:

$$\frac{\varepsilon M}{RT_g}\frac{\partial P_g}{\partial t}+\frac{\varepsilon MP_g}{R}\frac{\partial}{\partial t}\left(\frac{1}{T_g}\right)-\frac{1}{r}\frac{k}{\upsilon}\frac{\partial}{\partial r}\left(r\frac{\partial P_g}{\partial r}\right)-\frac{k}{\upsilon}\frac{\partial^2 P_g}{\partial z^2}-\frac{1}{r}\frac{k}{\upsilon}\frac{\partial^2 P_g}{\partial\theta^2}-(1-\varepsilon)\rho_s\frac{\partial X}{\partial t}=0 \tag{5}$$

The Linear Driving Force Model (LDFM), was used to describe the behaviour of the adsorption capacity rate with time; based on the LDFM, Glueckauf [41] proposed a formula to relate the rate of adsorption to diffusivity.

$$\frac{\partial X}{\partial t}=-G\left(X-X_{eq}\right) \tag{6}$$

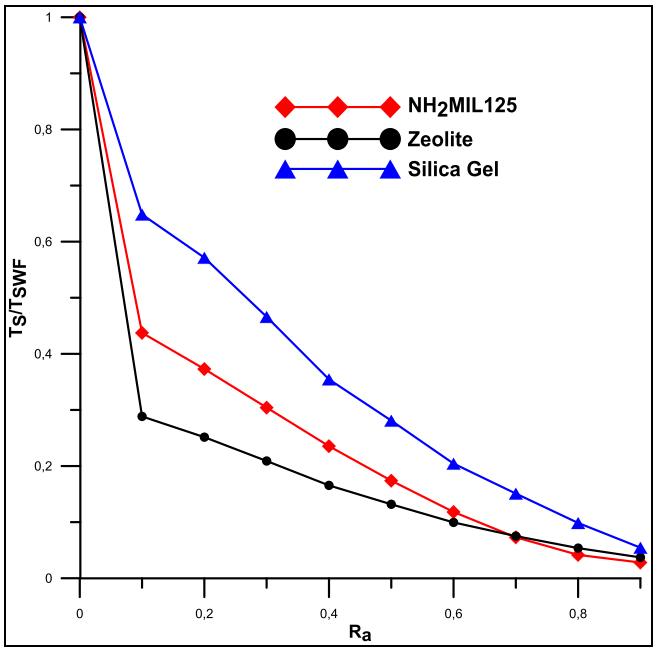

Fig. 9. Saturation time ratio against the R_a.

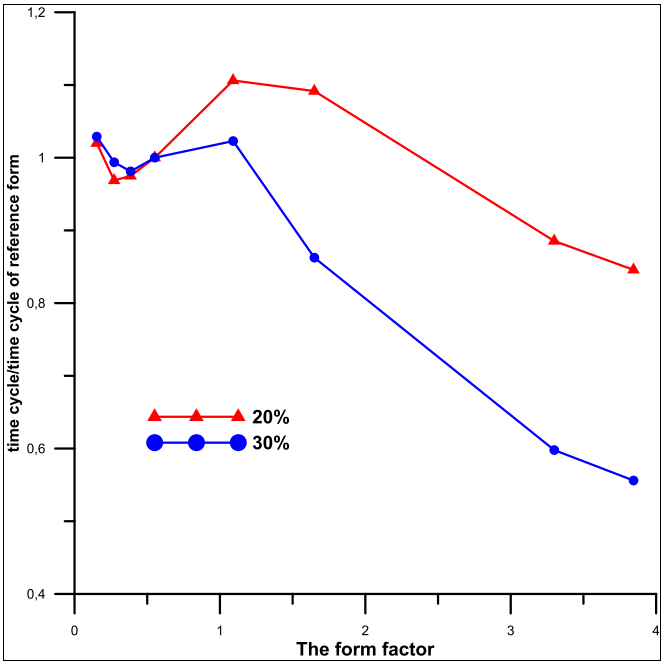

Fig. 10. Effect of the factor form (F) on the time cycle for two saturation values (20% and 30%).

Where G is the mass transfer coefficient:

$$G = \frac{15D_{eff}}{r_p^2} \tag{7}$$

$$D_{eff} = D_0 \exp\left(\frac{-E_a}{RT_g}\right) \tag{8}$$

D_{eff} is the effective diffusion coefficient.

The equilibrium adsorption capacity X_{eq} of Zeolite/water pair was evaluated by:

- *Using Dubinin equation as:*

$$X_{eq} = X_{in}\exp\left[-D\left(T_g \ln\left(\frac{P_{sat}(T_g)}{P_g}\right)\right)^2\right] \tag{9}$$

Where: X_{in} and D were given experimentally by Guilleminot [42]

- *Using Langmuir equation as:*

$$X_{eq} = \frac{X_{s1}b_1P_g}{1+b_1P_g} + \frac{X_{s2}b_2P_g}{1+b_2P_g} + \frac{X_{s3}b_3P_g}{1+b_3P_g} \tag{10}$$

Where:

$$X_{s1} = \sum_{i=0}^{3}\frac{a_i}{T^i} \tag{11}$$

$$X_{s2} = \sum_{i=0}^{3}\frac{c_i}{T^i} \tag{12}$$

$$X_{s3} = X_{in} - X_{s1} - X_{s2} \tag{13}$$

$$b_i = b_{0i}\exp\left(\frac{E_i}{T}\right) \tag{14}$$

The coefficients a_i, b_i, c_i and E_i (i = 1 to 3) are given in Table 1

The equilibrium adsorption capacity X_{eq} of silica gel/water pair is defined using Dubinin-Astakhov (D-A) equation Di et al [44]:

$$X_{eq} = 0.346\exp\left[-5.6(T_g/T_{sat})^{1.6}\right] \tag{15}$$

The equilibrium adsorption capacity X_{eq} of NH_2MIL125/water pair as the model for isotherm type V extended is given below [45]:

$$X_{eq} = \frac{1}{D}\left[\tan^{-1}\left(\frac{P/P_{sat} - A}{B}\right)G - \tan^{-1}\left(\frac{-A}{B}\right)\right]E - F \tag{16}$$

Where: A, B, E, F and G they are given in Table 2

Then D is calculated as follows:

$$D = \left[\tan^{-1}\left(\frac{1-A}{B}\right) - \tan^{-1}\left(\frac{-A}{B}\right)\right] \tag{17}$$

2.2.2. Energy conservation equations

The energy balance for fins is described as:

$$\rho_f C_{pf}\frac{\partial T_f}{\partial t} - div\left[\lambda_f \overrightarrow{grad(T_f)}\right] = 0 \tag{18}$$

In cylindrical coordinates, the expression is given as follows:

$$\rho_f C_{pf}\frac{\partial T_f}{\partial t} - \frac{1}{r}\frac{\partial\left(r\lambda_f\frac{\partial T_f}{\partial r}\right)}{\partial r} - \frac{1}{r^2}\frac{\partial\left(\lambda_f\frac{\partial T_f}{\partial \theta}\right)}{\partial \theta} - \frac{\partial\left(\lambda_f\frac{\partial T_f}{\partial z}\right)}{\partial z} = 0 \tag{19}$$

In the absence of local thermal equilibrium, the energy balance is given by:

- **For adsorbents**

$$\rho_s(1-\varepsilon)\left(C_{ps} + XC_{pg}\right)\frac{\partial T_s}{\partial t} = div\left[(1-\varepsilon)\lambda_s\overrightarrow{grad(T_s)}\right] + \dot{m}\Delta H_{vap} - H_{gs}S\left(T_g - T_s\right) \tag{20}$$

- **For Gas**

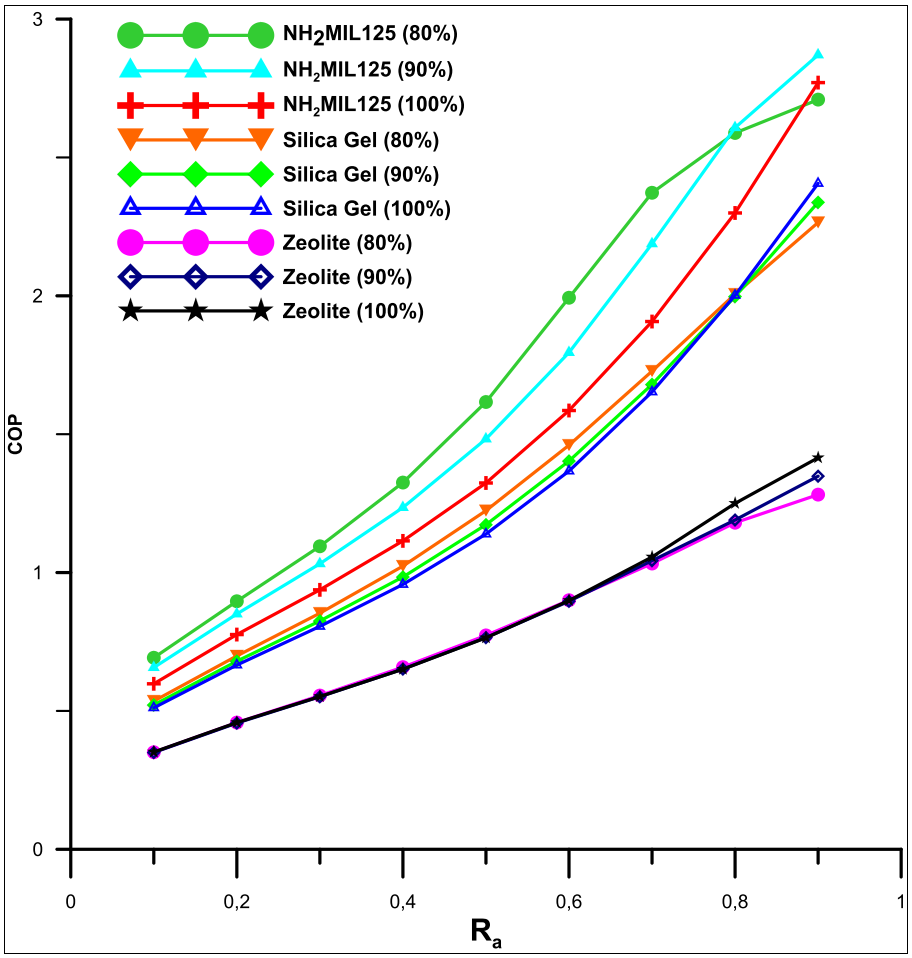

Fig. 11. Variation of COP three pairs for 100%, 90% and 80% vapor mass with Ra.

$$\varepsilon\rho_g C_{pg}\frac{\partial Tg}{\partial t}+\rho_g\overrightarrow{V}C_{pg}\overrightarrow{grad(Tg)}=div\left[\varepsilon\lambda_g\overrightarrow{grad(Tg)}\right]+\dot{m}C_{pg}\left(T_g-T_s\right)$$
$$-H_{gs}S\left(T_g-T_s\right) \quad (21)$$

2.2.3. Energy conservation equation for local thermal equilibrium

If the local thermal equilibrium is valid, it can be considered that $T_g = T_s = T$. In fact, the energy conservation equations of the adsorbent **(20)** and the gas **(21)** can be reduced to:

$$\left[\rho_s(1-\varepsilon)\left(C_{ps}+XC_{pg}\right)+\varepsilon\rho_g C_{pg}\right]\frac{\partial T}{\partial t}+\rho_g\overrightarrow{V}C_{pg}\overrightarrow{grad(T)}$$
$$=div\left[\lambda_{ef}\overrightarrow{grad(T)}\right]+\dot{m}\Delta H_{vap} \quad (22)$$

In cylindrical coordinates:

$$\left[\rho_s(1-\varepsilon)\left(C_{ps}+XC_{pg}\right)+\varepsilon\rho_g C_{pg}\right]\frac{\partial T}{\partial t}+\frac{1}{r}\frac{\partial\left(r\rho_g V_r C_{pg}T\right)}{\partial r}+\frac{\partial\left(\rho_g V_z C_{pg}T\right)}{\partial z}+\frac{1}{r}\frac{\partial\left(\rho_g V_\theta C_{pg}T\right)}{\partial\theta}=$$
$$\frac{1}{r}\frac{\partial\left(r\lambda_{ef}\frac{\partial T}{\partial r}\right)}{\partial r}+\frac{\partial\left(\lambda_{ef}\frac{\partial T}{\partial z}\right)}{\partial z}+\frac{1}{r^2}\frac{\partial\left(\lambda_{ef}\frac{\partial T}{\partial\theta}\right)}{\partial\theta}+\dot{m}\Delta H_{vap} \quad (23)$$

2.2.4. Initials conditions

Initially, the pressure, the temperature and the moisture content in the bed are assumed to be constants:

$$P_g(0,r,\theta,z)=P_i \quad (24)$$

$$T(0,r,\theta,z)=T_i \quad (25)$$

$$T_f(0,r,\theta,z)=T_i \quad (26)$$

$$X(0,r,\theta,z)=X_{in} \quad (27)$$

2.2.5. Boundary conditions

The pressure boundary conditions.

The pressure values on the inner surface ($r = R_{in}$) are constant

$$P_g(t,R_{in},\theta,z)=P_c \quad (28)$$

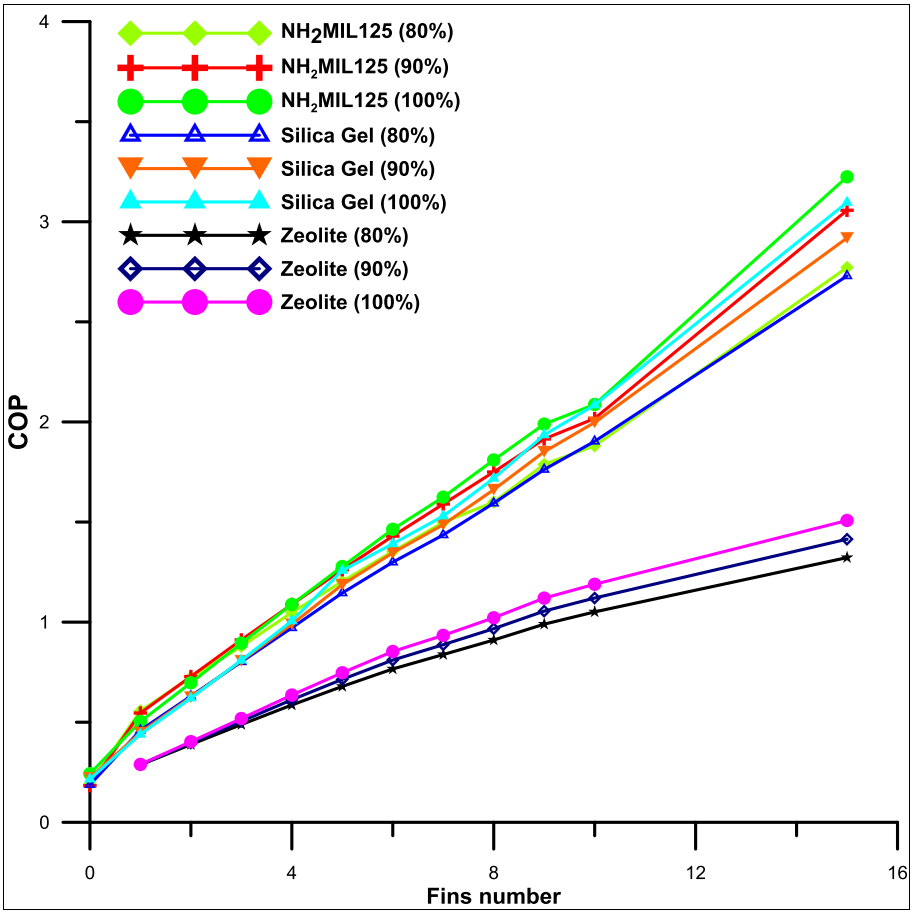

Fig. 12. Variation of COP of three pairs for 100%, 90% and 80% vapor mass with fins number.

$$\frac{\partial P_g(t,r,\theta,0)}{\partial z}=0 \tag{29}$$

$$\frac{\partial P_g(t,r,\theta,h)}{\partial z}=0 \tag{30}$$

$$\frac{\partial P_g(t,R_{ext},\theta,z)}{\partial r}=0 \tag{31}$$

$$\frac{\partial P_g(t,r,\theta,z_f)}{\partial z}=0 \tag{32}$$

The temperature boundary conditions

The boundary conditions of the adsorption chiller can be written as the follows:

$$-\lambda_{ef}\frac{\partial T(t,r,\theta,0)}{\partial z}=H(T-T_h) \tag{33}$$

$$-\lambda_{ef}\frac{\partial T(t,r,\theta,h)}{\partial z}=H(T-T_h) \tag{34}$$

$$-\lambda_{ef}\frac{\partial T(t,R_{ext},\theta,z)}{\partial r}=H(T-T_h) \tag{35}$$

$$-\lambda_{ef}\frac{\partial T(t,R_{in},\theta,z)}{\partial r}=0 \tag{36}$$

The boundary conditions between the porous media and vertical fins as the follows:

$$-\lambda_{ef}\frac{\partial T(t,r,\theta_f,z)}{\partial z}=-\lambda_f\frac{\partial T_f(t,r,\theta_f,z)}{\partial z} \tag{37}$$

$$-\lambda_{ef}\frac{\partial T(t,r_f,\theta_f,z)}{\partial z}=-\lambda_f\frac{\partial T_f(t,r_f,\theta_f,z)}{\partial z} \tag{38}$$

The boundary conditions between the porous media and horizontal fins, can be expressed as the follows

$$-\lambda_{ef}\frac{\partial T(t,r,\theta,z_f)}{\partial z}=-\lambda_f\frac{\partial T_f(t,r,\theta,z_f)}{\partial z} \tag{39}$$

$$-\lambda_{ef}\frac{\partial T(t,r_f,\theta,z_f)}{\partial z}=-\lambda_f\frac{\partial T_f(t,r_f,\theta,z_f)}{\partial z} \tag{40}$$

2.2.6. *Performance*

To evaluate the performance of the system, the performance coefficient and the specific cooling power were used.

The coefficient of performance is introduced as:

$$\mathrm{COP}=\frac{Q_{eva}}{Q_{ch}} \tag{41}$$

Where the total input heating (Qch) energy to the system is, calculated as:

$$Q_{ch}=\mathrm{H}^{*}\Delta\mathrm{S}^{*}\int_{t_1}^{t_3}(\mathrm{T}_{hf}-\mathrm{T}_i(\mathrm{t}))dt \tag{42}$$

Where: ΔS is convection exchange surface.

The cooling energy (Qeva) produced by the system is, calculated as:

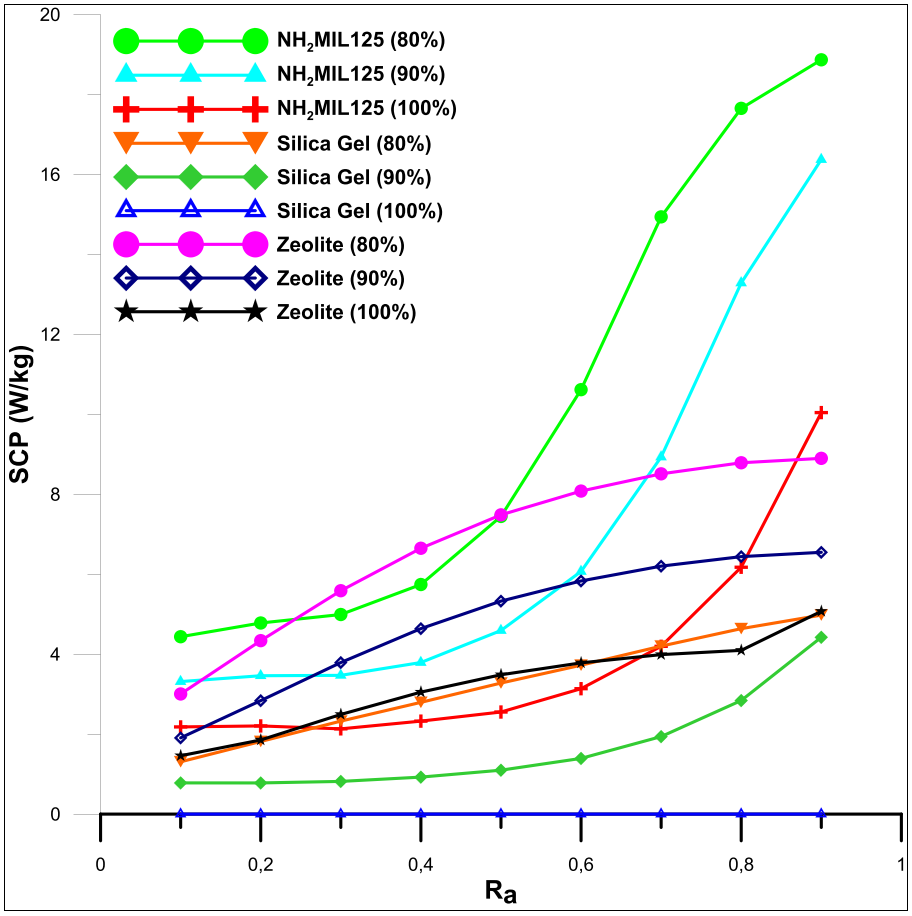

Fig. 13. Variation of SCP of three adsorbers for 100%, 90% and 80% vapor mass with Ra.

$$Q_{eva} = \int_{t_3}^{t_4} \left[L(T_{eva}) - \int_{T_{eva}}^{T_{cond}} C_{p,l}(T)dT \right] \dot{m} dt \quad (43)$$

where t_1 is the starting instant of the isosteric heating process while t_3, t_4, and t_5 are the instants of the isobaric heating, the isosteric cooling and isobaric cooling, respectively.

The Specific cooling power of the system is estimated as:

$$SCP = \frac{Q_{eva}}{t_c M_s} \quad (44)$$

Where M_s is the system mass and tc is cycle time.

2.2.7. Simulation method

The proposed numerical simulation for solving the equations of the above model is based on the Finite Volume Methods (FVM) [47].

Algebraic equations were discretized considering the following assumptions:

- The implicit scheme is adapted to the term which varies with time; the choice was made to avoid numerical instability, the implicit scheme is unconditionally stable;
- The convection terms are discretized by upwind scheme;
- The terms of accumulation and source terms are assumed constant in the control domain;
- The variations between neighboring nodes are linear; Discretize to first derivatives terms in space made by the centered scheme.

The iterative method is used to solve the obtained algebraic system of sweeping radial road line by line following the direction choice. This method is justified by the fast convergence regarding the iterative method point by point. In order to evaluate the calculated fields; in the beginning the simulation started with arbitrary values. For the resolution of the system of discretized equations, the method of the Gauss elimination was applicated. The convergence is reached when the values of the chosen arbitrary fields and the calculated solutions coincide.

For the simulation, Fortran 3D codes was developed. The grid points used depends on the design of the bed to have the same Δr and Δz values. For the standard bed (R_{out} = 10 cm, R_{int} = 7 cm and H = 30 cm) there is 300 points in z 140 points in r and 360 points for θ, the grid points number here 15120000. The computation time take about 144 h. Around the bed, the temperature is constant.

2.3. Model validation

To check the validity of our numerical model, the obtained numerical results are compared to those found by Mhimid [48] (Fig. 2). The simulation configuration is the same used by Mhimid; a cylindrical bed with a height equal to 1.2 m and an inner and outer radius equal to 0.03 m and 0.1 m, respectively. The experimental temperatures values on the outer lateral area, are used as the heat source temperature T_h during desorption phase. The condenser temperature (T_c) and pressure (P_c) are respectively equal to 313 K and 70 mbar. Fig. 3 shows a diamond-shaped curve presenting the experimental temperature on the outer surface of the adsorber (the heating temperature) measured experimentally by A. Mhimid [48]. This temperature is taken as the heating temperature of the adsorber in the simulation. The dotted line shows the temperature at which the adsorber heats up in our simulation. The dotted line shows the temperature at the inner surface measured experimentally and the two red and blue lines show the two curves resulting from our simulation on the inner surface of the adsorber as a function of the two models

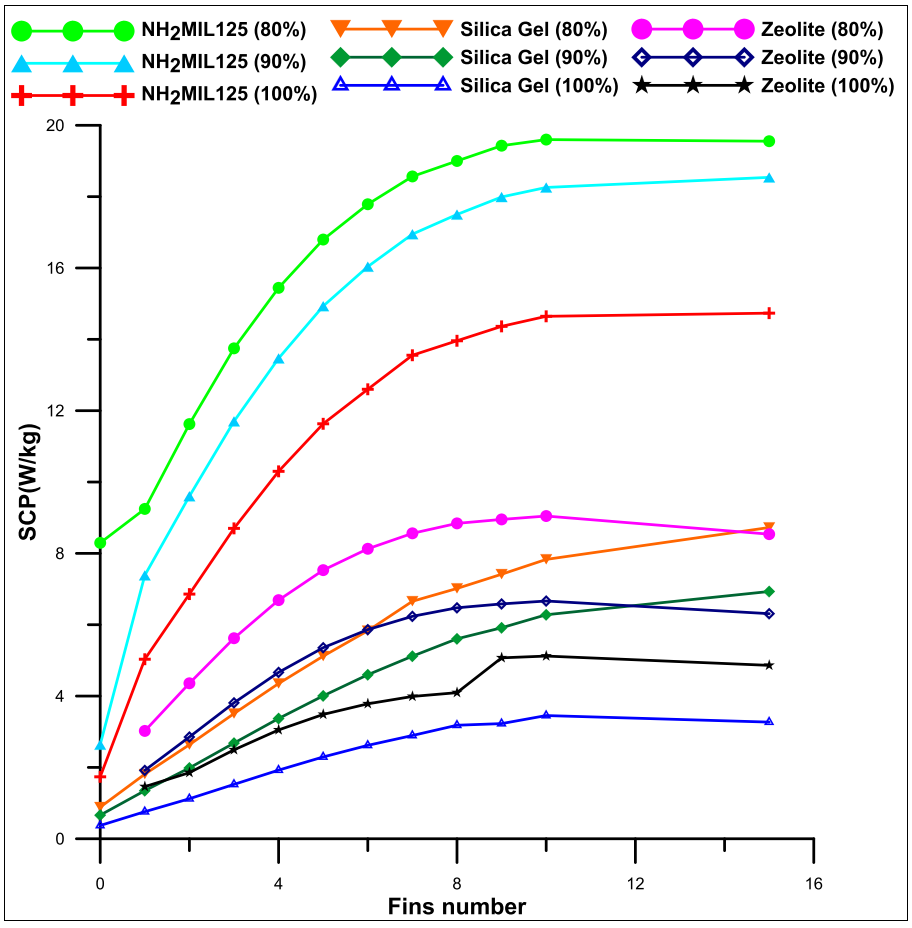

Fig. 14. Variation of SCP of three adsorbents 100%, 90% and 80% vapor mass with fins number.

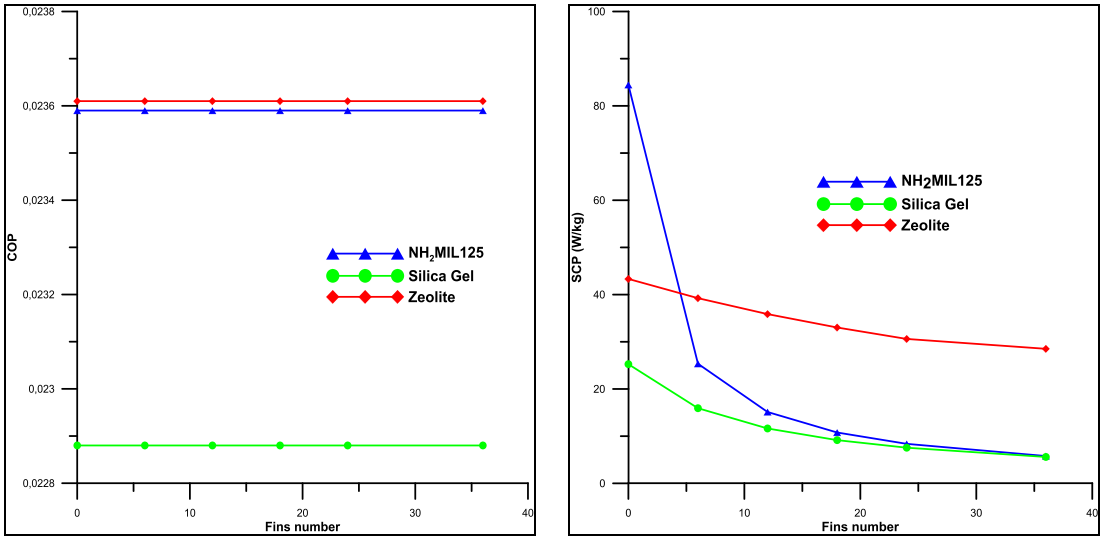

Fig. 15. Effect of fins number on COP and SCP for the three adsorbents.

indicated. The temperature curve shows good agreements and therefore the numerical methods are reliable and accurate.

The curves in Fig. 3 show the time evolution of the mass desorbed quantity profile, using both Dubinun and Langmier methods, in comparison with the experimental results found by Mhimid [48,49]. Hence, the mass desorbed graphs fit the results presented in literature. The quantity of the mass desorbed is increased with the time, reaching a peak of 750 g at 22000 s. This evolution is characterized by its unsteady increase. In fact, for the first 5000 s, the amount of accumulated desorbed mass is about 100 g. However, for the two following phases (5000 s−10000 s and 10000 s−15000 s), the amount of accumulated desorbed mass is above 250 g, with a decrease reaching100g at the last phase (15000 s-20000 s).

The checking of both Langmuir and Dubinin numerical model val-

idity needs also the examination of the mean error deviation for both temperature and mass desorbed graphs. In fact, the mean error formula used is expressed as follows:

$$\text{MeanError}(\%) = \frac{1}{N}\sum_{i=1}^{N}\frac{|Y_i - X_i|}{Y_i} \times 100 \quad (48)$$

Where: N is the total number values, Y_i is the temperature or mass desorbed found by experimental results from literature and X_i is the temperature or mass desorbed calculated by ours model. Table 3 summarizes the deviation of the results of the numerical models compared to those presented in literature. It shows maximum deviation of 1.71 % for temperature and 8.93 % for mass desorbed. The suitability of the numerical model has been demonstrated by this small deviation to simulate the heat and mass transfer.

3. Results and discussion

In this study, three couples were used: zeolite/water, silica gel/water and MIL125/water. The physical model and kinetic parameters of adsorption are described in the previous section. The values of the specific heat of adsorption for the couples used are 836 $Jkg^{-1}K^{-1}$ and 924 $Jkg^{-1}K^{-1}$ respectively for zeolite [48,31] and silica gel [24]. For $MIL125NH_2$, the value used is 1000 $Jkg^{-1}K^{-1}$, which is the average value of the average specific heat in the working temperature range [40].

3.1. Effect of fins number

The effect of the fins number implanted in the adsorber, on the kinetics of desorption phase with modification of parameters is studied. The fins number is varied from 1 to 15 for horizontal fins and from 2 to 36 for the vertical fins; the R_{in} is equal to 3 cm, R_{out} is equal to 13 cm and 30 cm height without fins. The height is varied to have the same amount of Zeolite in the adsorber. Fig. 4 shows radial sections of the adsorber with vertical fins taken respectively in the middle of the adsorber with different vertical fins number (5, 10 and 15) and different times (60 s, 900 s, 1800 s and 3600 s). Fig. 5 present spatio-temporal temperature profile in a finless adsorber and with 8 horizontal fins (for t = 60 s,3600 s, 5400 s, 7200 s,14400 s). The Fig. 4 and Fig. 5 show the evolution of the adsorption bed temperature during the preheating and desorption phases, considering a homogeneous initial temperature equal to the discharge temperature ($T_{ini} = T_{rej} = 296$ K). The increase of the exchange surface by increasing n (fins number) shows a better thermal diffusion.

For an adsorber equipped with horizontal fins, the evolution of the desorbed mass as a function of time is shown in Fig. 6. Different number of fins number are considered (1, 3, 6, 9 and 15). The figure shows that the difference in kinetics for this size of reactor gets higher with an increase of the number of fins from 1 to 6. However, this difference becomes smaller for numbers of fins more than 6.

The effect of the fins numbers on desorption kinetics is evaluated considering three adsorbent (Zeolite, silica gel and MIL125) the same configuration is used.

The quantity of the adsorbent is fixed to have the same maximum amount of desorbed vapor. A dimensionless parameter φ is considered. This parameter is defined as the ratio between the saturation times of reactor with fins T_{sat} by the saturation time of the reactor without fins T_{swf}. It can be expressed as follows:

$$\varphi = T_{sat}/T_{swf} \quad (49)$$

Fig. 7 showed that φ declined when the fins number augmented. In fact, after planting the first horizontal fin (Fig. 7 (a)) and six vertical fins (Fig. 7 (b)), the saturation time of Zeolite, MIL125 and silica gel decreases, respectively, to 0.179, 0.278 and 0.412 for horizontal fins and to 0.44, 0.59 and 0.71 for vertical fins in comparison to the saturation time of the three adsorbents without fins.

In the horizontal fins design, for the Zeolite, φ decreases to reach a value equal to 0.02 after the fifth fins. Meanwhile for the MIL125 and Silica Gel, φ reaches a value of 0.02 respectively after the seventh and the eighth fins.

For the vertical fins design, φ was dropping after adding 12 fins for the three adsorbents. From n = 18, φ is showing is slightly decrease and almost having a stable value which is around 0.086 for Zeolite and 0.095 for NH_2MIL125. While the dimensionless parameter φ, for the silica gel, starts to be stable after adding 24 fins to be around 0.11.

This difference is due to the conductivity parameter value of the different materials type. Moreover, for the same adsorber configuration, the highest conductivity value causes the decrease of the sensibility of the fins additions.

3.2. Effect of fins radius

To study the effect of the fin's radius on the heat exchange and then on the kinetic desorption, a dimensionless radius parameter R_a is considered. It is defined as follows:

$$R_a = \frac{R_f}{R_{out} - R_{in}} \quad (50)$$

Where: R_f, R_{out} and R_{in} are the fin radius, the outer tube radius, and the mass transfer tube radius, respectively.

Fig. 8(a) shows the effect of R_a on the Zeolite/water torque desorption kinetics. In fact, the outer tube radius, mass transfer tube radius and fins number are kept constant (R_{out} = 10 cm, R_{in} = 3 cm and fins number = 15), the adsorber height is varied to conserve the amount of the mass desorbed and the R_a parameter is varied from 0.1 to 0.9. It is interesting to note the existence of a significant effect on desorbed mass. It is more pronounced for high values of R_a. Indeed, the R_a increment from 0.1 to 0.9 gives a gain approximately equal to 150,000 s for the desorption kinetics of the Zeolite/water. Fig. 8**(b)** shows the evolution of X average adsorbed amount (kg/kg) (R_a = 0.9, 0,6 and 0,1with 15 vertical fins) for MIL125 NH_2 /water. the figure shows a very slight difference between the three curves (almost merging). The effect of the radius of the vertical fins is negligible for this adsorber configuration.

To study the effect of the time saturation ratio φ for the three adsorbents Fig. 9 shows the evolution of φ of this parameter when the total mass desorbed equals 80 %. φ is presented against the size of the fins. The sensitivity to the increase of the fins area, according to three adsorbents, depends on their thermal conductivities. The increase of the fins size leads to this ratio. For the cases of NH_2-MIL125 and Zeolite, for R_a = 0.6, the variation of φ is negligible, almost of 0.03. Therefore, a lowering in terms of the mass of the reactor is observed. Nevertheless, for the case of Silica Gel, the optimization of the fins size is obtained for a value of R_a = 0.9.

3.3. Effect of the form factor

To study the effect of the adsorber design on the heat and mass transfer, the factor form has been evaluated. An adsorber filled with NH_2MIL125 using 15 vertical fins has been used and the radius and the height were variable.

The factor form (**F**) is dimensionless (the fraction of the lateral surface by the longitudinal surface of the adsorber). Fig. 10 shows the effect of the factor form on fraction of the saturation time/the saturation time of the reference form (R_{int} = 0.03, R_{ex} = 0.1 and h = 0.3) saturation values (20 % and 30 %) of maximal adsorbed mass. The two curves are characterised by three phases.

In the first phase F < 0.4, which corresponds to low F value, the ratio decreases from 1.03 till a limit of 0.97 because in the beginning the heat transfer is one-dimensional and depend only on z. When F rises, the radius is diminished, and the effect of the vertical fins became

significant. In the second phase $0.4 < F < 1.1$, when F increases r is reduced, and h is augmented. The resistance (Inertia) is improved, and the saturation time is expanded. In the third phase when $F > 1.1$, the height is increased, and the radius is dropped significantly. The inertia becomes low, and the vertical fins effect turns out to be higher. So, the heat transfer is becoming so important, and the saturation time is lowering.

3.4. COP and SCP

3.4.1. Horizontal fins

To study the fins radius effect, the same simulation conditions are adapted. Fig. 11 shows the effect of the radius of the fins on the COP for different amount of desorbed mass. The three adsorbents show almost a linear increase of the COP, as a function of the radius of fins, from: 0.51 to 2.40 for the silica gel, 0.35 to 1.41 for the zeolite and 0.6 to 2.89 for NH_2-MIL125, when R_a varies from 0.1 to 0.9. It is noted that the COP of the two couples' silica gel/water and zeolite are independent of the mass rate used. On the other hand, for NH_2-MIL125, between $R_a = 0$ and 0.7, the COP is higher for a mass 80 % of the maximum mass and the COP of 90 % is greater than 100 %. From $R_a = 0.8$, the profile of the NH_2-MIL125 curve is reversed.

Fig. 12 shows the evolution of the COP as a function of the number of fins for the three adsorbers. The COP is between 0.2 and 3 for the silica gel/water pair and 0.3 and 1.55 for the couple Zeolite/ water. Results also show that the COP has a linear trending in function of number of fins. The evolution due to the decrease of the input het energy Q_{ch} with the rise of the number of fins.

As it is known, the COP does not present a criterion of the determining choice. Specifically, the Specific Cooling Capacity (SCP) has an important criterion for the choice of an adsorber of optimal yield as a function of weight. Fig. 13 shows the evolution of mass SCP of the three pairs as a function of fins radius. Unlike the COP, the SCP profiles of the three couples are different. For the silica gel/water pair, Fig. 13 shows three different speeds depending on the percentage of mass. For a mass of refrigerant equal to the maximum adsorbed mass, the SCP is very low of the order of 1/10000 is these values are due to the very long cycle of silica gel/water. For a percentage of 90 %, the curve of the SCP as a function of R_a has two parts, between $R_a = 0.1$ and 0.5, the SCP varies slightly. Nevertheless, between 0.91 and 1.05 the SCP varies exponentially to reach 4.5. For the 80 % curve, the SCP profile varies linearly between 1.46 and 4.98. For the zeolite/water pair as a function of Ra, the three curves present at the beginning a linear profile up to $R_a = 0.6$. From this value, the curves start to have saturation, whose SCP values are 8.9 for 80 % of the mass desorbed, 6.6 for 90 % and 4.5 for 100 %. Indeed, for the NH_2-MIL125/water pair, the three SCP curves has a constant profile up to $R_a = 0.5$. From this value the SCP starts to increase to a saturation value. The figure shows that for our adsorber and for values of R_a between 0.2 and 0.5, the zeolite at 80 % of the desorbed mass has the favorable adsorbent with a very slight difference of NH_2-MIL125. For the other values of Ra, NH_2-MIL125 has very important values in terms of the SCP up to 2 times of zeolite and 4 times the silica gel. Fig. 14 shows the evolution of the SCP as a function of the number of fins for the three pairs. The SCP of the silica gel/water pair improves with the increase of the number of fins. For the case where the mass of the refrigerant equal to the maximum mass adsorbed, the SCP reaches an optimal value before it begins to decrease with the increase in the number of fins. The SCP of the two pairs Zeolite/water and NH_2-MIL125 behaves in the same way between 0 and 15 fins. At the beginning a gradual increase of 3.02 for the zeolite and 8.29 for the NH_2-MIL125 up to an optimal value of about 0.94 for the zeolite and 19.25 for NH_2-MIL125. At the end, the profile of the SCP is degrading with increasing number of fins. Both pairs have optimal SCP values for a number equal to 10 fins and a percentage of 80 % of the total adsorbed mass. For the same adsorber, the same geometry and with the same desorbed-adsorbed mass of water vapor (refrigerant) (Fig. 14), NH_2-MIL125 has SCP values twice as large as silica gel and zeolite. From both Fig. 12 and Fig. 14 the optimal configuration for our prototype is reached for equal numbers of fins 9 and 10 for a percentage of 80 % of the maximum.

3.4.2. Verticals fins

Results (Fig. 15) show that the COP has a constant low value (0.024) without optimisation. COP is not depending to fins number. When the fins number is getting higher the heat transfer is slightly improved. Augmenting the fins number gives a significant increase of the adsorber mass and decreases slightly the cycle time. For those reasons, the SCP is declined. NH_2-MIL125 has the highest SCP value (80 Wh/kg) comparing to Zeolite and Silica Gel. From the number of 12 fins, the Silica Gel has the important SCP value which is almost the double of the values for the Zeolite and NH_2-MIL125.

These results are due to the factor form of our design used in the second zone (Fig. 10). For this zone the horizontal fins are more efficient than the vertical fins.

4. Conclusion

A 3D numerical model was developed using Fortran. It was used to study heat and mass transfer during the desorption phase in a cylindrical adsorber in the presence and absence of fins (vertical or horizontal). Three different adsorbent-adsorbate pairs were considered (water-zeolite, water–silica gel and water-NH2MIL125). The main conclusions obtained are:

(1) In desorption phase, the results prove that the sensibility of the fins addition decrease with the increase of thermal conductivity of adsorbents. The sensitivity of saturation time for the radius effect is linear.
(2) For the same desorption quantity, the NH_2-MIL125 the optimal adsorbent due to the adsorption capacity and conductivity.
(3) The factor form F is correlated to the time cycle and the heat transfer. F has an optimal value of 0.4 when the number of fins is 15.
(4) For the horizontal fins, the decreases of COP values increasing of fins numbers due to the decrees of Q_{ch} quantity. Increasing the fins numbers decrease the COP values. Increasing the radius fins decrease the COP values. Decreasing the mass of vapor, used in during the adsorption cycle, increase the SCP values. The SCP of NH_2-MIL125 presents the best values.
(5) The NH_2-MIL125 presents a promising adsorbent for the adsorption cooling system.
(6) For the verticals fins, the coefficient of performance (COP) shown to be independent from the fins number. The Specific Cooling Power (SCP) is affected by the fins number of the three adsorbents. NH_2-MIL125 is giving the best result of SCP reaching a value of 80 Wh/kg.
(7) There is no optimal value of fins number because of the factor form of the configuration reference which is about 0.6. The effect of the vertical fins number became higher for a factor form values below 0.4 or above 1.1.

CRediT authorship contribution statement

Oussama Ayed: Conceptualization, Data curation, Writing – original draft, Visualization, Investigation, Validation, Writing – review & editing, Formal analysis, Methodology. **Sébastien Thomas:** Writing – original draft, Supervision. **Philippe Andre:** Methodology, Supervision. **Abdelmajid Jemni:** Methodology, Writing – review & editing, Formal analysis, Supervision.

Declaration of competing interest

The authors declare that they have no known competing financial

interests or personal relationships that could have appeared to influence the work reported in this paper.

Data availability

Data will be made available on request.

References

[1] M. Kilic, M. Anjrini, Comparative performance analysis of a combined cooling system with mechanical and adsorption cycles, Energy Conversion Manage. 221 (2020) 113208.

[2] J.A. Edmonds, DL. Wuebles, MJ Scott. Energy and radiative precursor emissions. In: Proceedings of the 8th Miami international conference on alternative energy sources.14–16 December1987.

[3] A. Shirazi, R.A. Taylor, G.L. Morrison, S.D. White, A comprehensive, multi-objective optimization of solar-powered absorption chiller systems for air-conditioning applications, Energy Convers. Manage. 132 (2017) 281–306.

[4] J. Wang, E. Hu, A. Blanzewizc, A.W. Ezzat, Simulation of accumulated performance of a solar thermal powered adsorption refrigeration system with daily climate conditions, Energy 165 (2018) 487–498.

[5] A.A. Askalany, M. Salem, I.M. Ismael, A.H.H. Ali, M.G. Morsy, B.B. Saha, An overview on adsorption pairs for cooling, Renew. Sustain. Energy Rev. 19 (2013) 565–572.

[6] P.S. Ramesh, B. Choudhury, K.D. Ranadip, A review on heat powred adsorption cooling systems for ice production, Renewable Energy Reviews 62 (2016) 109–120.

[7] A.H. Poshtiri, S. Bahar, A. Jafari, Daily cooling of one-story buildings using domed roof and solar adsorption cooling system, Appl Energy 182 (2016) 299–319.

[8] A.A. Hassan, A.E. Elwardany, S. Ookawara, M. Ahmed, I.I. El-Sharkawy, Integrated adsorption-based multigeneration systems: a critical review and future trends, Int. J. Refrig. 116 (2020) 129–145.

[9] A.A. Hassan, A.E. Elwardany, S. Ookawara, H. Sekiguchi, H. Hassan, Performance and economic analysis of hybrid solar collectors-powered integrated adsorption/reverse osmosis multigeneration system, Int. J. Energy Res. (2022) 1–24.

[10] C. Forman, I.K. Muritala, R. Pardemann, B. Meyer, Estimating the global waste heat Potential, Renew. Sustain. Energy Rev. 57 (2016) 1568–1579.

[11] A.A. Hassan, H. Hassan, M.A. Islam, B.B. Saha, Thermoeconomic performance assessment of a novel solar-powered high temperature heat pump/adsorption cogeneration system, Sol. Energy 255 (2023) 71–88.

[12] A.A. Hassan, A.E. Elwardany, S. Ookawara, I.I. El-Sharkawy, Performance investigation of a solar-powered adsorption-based trigeneration system for cooling, electricity, and domestic hot water production, Appl. Therm. Eng. 199 (2021) 117553.

[13] A.J. Rieth, A.M. Wright, S. Rao, H. Kim, A.D. LaPotin, E.N. Wang, et al., Tunable metalorganic frameworks enable high efficiency cascaded adsorption heat pumps, J. Am. Chem. Soc. 140 (50) (2018) 17591–17596.

[14] A.A. Askalany, S.J. Ernst, P.P.C. Hugenell, H.J. Bart, S.K. Henninger, A.S. Alsaman, High potential of employing bentonite in adsorption cooling systems driven by low grade heat source temperatures, Energy 141 (2017) 782–791.

[15] B. Choudhury, B.B. Saha, P.K. Chatterjee, J.P. Sarkar, An overview of developments in adsorption refrigeration systems towards a sustainable way of cooling, Appl. Energy 104 (2013) 554–567.

[16] J. Li, M. Kubota, F. Watanabe, N. Kobayashi, M. Hasatani, Optimal design of a fin-type silica gel tube module in the silica gel/water adsorption heat pump, J. Chem. Eng. Jpn. 37 (4) (2004) 551–557.

[17] K.C. Leong, Y. Liu, Numerical modeling of combined heat and mass transfer in the adsorbent bed of a zeolite/water cooling system, Appl Therm Eng 24 (2004) 2359–2374.

[18] D.C. Wang, Z.Z. Xia, J.Y. Wu, R.Z. Wang, H. Zhai, W.D. Dou, Study of a novel silica gel-water adsorption chiller. Part I. Design and Performance Prediction, Int. J. Refrigeration. 28 (2005) 1073–1083.

[19] M. Kubota, T. Ueda, R. Fujisawa, J. Kobayashi, F. Watanabe, N. Kobayashi, M. Hasatani, Cooling output performance of a prototype adsorption heat pump with fin-type silica gel tube module, Appl. Therm. Eng. 28 (2008) 87–93.

[20] L.Z. Zhang, L. Wang, Effects of coupled heat and mass transfers in adsorbent on the performance of a waste heat adsorption cooling unit, Appl. Therm. Eng. 19 (1999) 195–215.

[21] B.B. Saha, A. Chakraborty, S. Koyama, Y.I. Aristov, A new generation cooling device employing CaCl2-in-silica gel-water system, Int. J. Heat. Mass Tran. 52 (1–2) (2009) 516–524.

[22] Y. Pei-zhi, Heat and mass transfer in adsorbent bed with consideration of non-equilibrium adsorption, Appl. Therm. Eng. 29 (2009) 3198–3203.

[23] H. Niazmand, I. Dabzadeh, Numerical simulation of heat and mass transfer in adsorbent beds with annular fins, Int. J. Refrigeration. 35 (2012) 581–593.

[24] H. Niazmand, H. Talebian, M. Mahdavikhah, Bed geometrical specifications effects on the performance of silica/water adsorption chillers, Int. J. Refrigeration. 35 (2012) 2261–2274.

[25] K. Grabowska, M. Sosnowski, J. Krzywanski, K. Sztekler, W. Kalawa, A. Zylka, W. Nowak, The numerical comparison of heat transfer in a coated and fixed bed of an adsorption chiller, Journal of Thermal Science. 27 (5) (2018) 421–426.

[26] K. Grabowska, J. Krzywanski, W. Nowak, M. Wesolowska, Construction of an innovative adsorbent bed configuration in the adsorption chiller-Selection criteria for effective sorbent-glue pair, Energy. 151 (2018) 317–323.

[27] X. Song, X. Ji, M. Li, Q. Wang, Y. Dai, J. Liu, Effect of desorption parameters on performance of solar water-bath solid adsorption ice-making system, Appl. Therm. Eng. 89 (2015) 316–322.

[28] Z. Rogala, Adsorption chiller using flat-tube adsorbers–Performance assessment and optimization, Appl Therm Eng 121 (2017) 431–442.

[29] M. Verde, K. Harby, J.M. Corberán, Optimization of thermal design and geometrical parameters of a flat tube-fin adsorbent bed for automobile air-conditioning, Appl Therm Eng 111 (2017) 489–502.

[30] M.M. Kowsari, H. Niazmand, M.M. Tokarev, Bed configuration effects on the finned flat-tube adsorption heat exchanger performance: Numerical modeling and experimental validation, Appl. Energy (2017).

[31] B. Golparvar, H. Niazmand, A. Sharafian, A.A. Hosseini, Optimum fin spacing of finned tube adsorber bed heat exchangers in an exhaust gas-driven adsorption cooling system, Applied Energy. 232 (2018) 504–516.

[32] L. Ye, M.A. Islam, T.H. Rupam, I. Jahan, B.B. Saha, Study on the adsorption characteristics of Maxsorb III/HFO-1234ze(E) pair for adsorption refrigeration applications, Int. J. Refrigeration. 146 (2023) 248–260.

[33] Y.I. Aristov, I.S. Glaznev, A. Freni, G. Restuccia, Kinetics of water sorption on SWS-1L (calcium chloride confined to mesoporous silica gel): influence of grain size and temperature, Chem. Eng. Sci. 61 (2006) 1453–1458.

[34] H. Kakiuchi, S. Shimooka, M. Iwade, T. Takewaki, Novel water vapor adsorbent FAM-Z01 and its applicability to an adsorption heat pump, J. Chem. Eng. Jpn. 31 (5) (2005) 361–364.

[35] H. Kakiuchi, S. Shimooka, M. Iwade, T. Takewaki, Water vapor adsorbent FAMZ02 and its applicability to adsorption heat pump, J. Chem Eng Jpn. 31 (4) (2005) 273–277.

[36] T.H. Rupam, F.J. Tuli, I. Jahan, M.L. Palash, A. Chakraborty, B.B. Saha, Isotherms and kinetics of water sorption onto MOFs for adsorption cooling applications, Therm. Sci. Eng. Prog. 34 (2022) 101436.

[37] T.H. Rupam, T. Steenhaut, M.L. Palash, Y. Filinchuk, S. Hermans, B.B. Saha, Thermochemical energy applications of green transition metal doped MIL–100(Fe) T, Chem. Eng. J. 448 (2022) 137590.

[38] I. Jahan, M.A. Islam, T.H. Rupam, M.L. Palash, K.A. Rocky, B.B. Saha, Enhanced water sorption onto bimetallic MOF-801 for energy conversion applications, Sustain. Mater. Technol. 32 (2022) e00442.

[39] S.N. Kim, J. Kim, H.Y. Kim, H.Y. Cho, W.S. Ahn, Adsorption/catalytic properties of MIL-125 and NH_2-MIL-125, Catal Today. 204 (2013) 85–93.

[40] L.G. Gordeeva, M.V. Solovyeva, Y.I. Aristov, NH2-MIL-125 as a promising material for adsorptive heat transformation and storage, Energy. 100 (2016) 18–24.

[41] E. Glueckauf, Theory of chromatography. Part 10.—Formulæ for diffusion into spheres and their application to chromatography, Trans. Faraday Soc. 51 (1955).

[42] J.J. Guilleminot, Caracterisation de l'etat stationnaire liquide-gaz adsorbant lors de l'adsorption de gaz condensable sur le zeolithes These de doctorat, Universite de Dijon, Dijon (France), 1978.

[43] N. Ben Amar, L.M. Sun, F. Meunier, Numerical analysis of adsorptive temperature wave regenerative heat pump, Appl. Therm. Eng 16 (1996) 405–418.

[44] J. Di, J.Y. Wu, Z.Z. Xia, R.Z. Wang, Theoretical and experimental study on characteristics of a novel silica gelwater chiller under the conditions of variable heat source temperature, Int. J. Refrig. 30 (2007) 515–526.

[45] J.J. Mahle, An adsorption equilibrium model for Type 5 isotherms, Carbon 40 (2002) 2753–2759.

[46] G.I. Gamze, Influence of new adsorbents with isotherm Type V on performance of an adsorption heat pump, Energy. 119 (2017) 86–93.

[47] S. Patankar, Numerical Heat Transfer and Fluid Flow, McGraw-Hill Company, New York, 1980.

[48] A. Mhimid, Theoretical study of heat and mass transfer in a zeolite bed during water desorption: validity of local thermal equilibrium assumption lnt, J. Heat Transfer. 41 (1998) 2967–2977.

[49] A. Mhimid, Etude expérimentale de la réfrigération solaire par adsorption utilisant des capteurs à zéolithe, plans et à concentrations. Thèse De Doctorat De Spécialité De L'université De Tunisie, 1991.